SAND95-1708C

Computing the Apparent Centroid of Radar Targets

Cullen E. Lee

Sandia National Laboratories
Dept. 9835, MS 0105
Albuquerque, NM 87185-0105

Ph. (505)-844-5802
FAX (505)-844-9895

1 Introduction

A tracking radar system attempts to track the physical centroid of a target by first sensing the phase fronts of the electromagnetic field scattered by the target and then determining the phase gradient associated with the scattered field. The phase gradient of the scattered field, being normal to the phase front, is used to estimate the direction to the target. An intuitive basis for such a tracking paradigm is provided by the scalar field point target. In that case the phase fronts are spherical in shape and yield exact target direction information. The implication for complex targets is that the phase gradient (hopefully) points in the direction of the target centroid. However, wave scattering from a complex target usually results in a highly superimposed field. Resulting in significant phase front deviation relative to that of a simple point target. Such deviation can be extreme and result in significant tracking error. These errors degrade performance of the tracking system and are said to be caused by glint.

Glint induced tracking errors result from the interference effects that occur within the field scattered from an extended target. These interference effects cause the apparent radar centroid (ARC) of the target, i.e., the centroid computed from the scattered field data, to no longer be coincident with its physical centroid. It has been well known for several decades that the magnitude of such errors can fall well outside the physical bounds of the target. In fact, the first statistical analysis of glint induced tracking errors [1] suggested that this was the case 13.4% of the time. In modern tracking radar systems glint effects are the limiting factor in tracking performance. As such, a great deal of attention has been given to understanding glint phenomenology and reducing its affect on tracking systems, [2].

Over the past four decades there have been many glint models developed. These models generally fall into one of two categories: (i) statistical models, see [1, 3-6] and (ii) discrete scatterer models, see [7-9]. The statistical models are parametric by design and require one to make a number of assumptions concerning the location, strength, and statistical dependence of the scattering centers. On the other hand, the discrete scatterer model requires one to have knowledge of the location and strength of every scattering center associated with a given target, of which there may be thousands. To further confound the discrete scatterer model, the ensemble of scattering centers can change quite rapidly as a function of aspect angle. Perhaps this is the reason that statistical models have been chosen almost exclusively over discrete scatter models for determining glint behavior. Unfortunately, statistical models can give very little, if any, information on glint behavior for specific targets of interest. To overcome this inherent deficiency requires the introduction of target specific scattering data into the statistical model, [6]. Of course if target specific scattering data are not available, then the deficiency remains.

The development of more sophisticated computing platforms allows one to revisit the methods and procedures used for computing radar scattering from electrically large targets, [10]. In particular, it enables one to reconsider using the discrete scatterer approach when determining the glint errors associated with specific targets of interest. In this paper, a discrete scatterer model will be developed and used to study target specific tracking errors resulting from glint. Several examples will be given illustrating how the ARC of a specific target wanders in an endgame engagement.

2 Defining the Apparent Centroid of a Radar Target

The discrete scatterer model assumes the signal appearing at the terminals of a tracking systems receiving antenna can be well represented by the superposition of a finite number of complex sinusoids. To each complex sinusoid one associates a scattering center, appropriately located in R^3. The ensemble of scattering centers needed to well represent the received signal will necessarily depend upon the geometric configuration of the target and tracking system, Fig. 1. Hence, each time this configuration changes, the scattering center ensemble must be reconstructed. The position of the n^{th} scattering center is taken to be (x_n, y_n, z_n) and the associated complex sinusoid is $e_n = E_n \exp(i\phi_n)$. The complex amplitude U of the received signal is just the superposition of the complex sinusoids at the receiver location, defined to be the point $P(x, y, z)$.

$$U(P) = \sum_n e_n \tag{1}$$

Each scattering center e_n will now depend not only on the geometric configuration of the target and tracking system, but also on the operating characteristics of both the transmitter and receiver portions of the tracking system, e.g., the operating frequency, antenna patterns, and polarization.

The physical centroid of the target is taken to be at the origin. However, the ARC of the target is determined using the ensemble of scattering centers and will vary as the ensemble changes. To determine the ARC of this ensemble one must first determine the phase gradient of the complex amplitude U. If the complex amplitude is expressed as $U = |U| \exp(i\Phi_U)$, then the phase gradient of U can be readily determined.

$$\nabla\Phi_U = P^{-1}\mathrm{Im}\,[\tilde{U}\nabla U] \tag{2}$$

where $\tilde{U}$ is the complex conjugate of U and $P = \tilde{U}U$ is the power contained in the received signal.

An algorithmic form for the phase derivative can be obtained by inserting eqn. 1 in eqn. 2 and using the fact that the spatial dependence of the phase is $\phi_n = kR_n$, where $R_n = |\bar{r} - \bar{s}_n|$ and k is the free-space wave number. The expression for the phase gradient becomes

$$\nabla\Phi_U = P^{-1}\left[\sum_{m,l} E_m(\nabla E_l)\sin(\phi_l - \phi_m) + k\sum_{m,n} E_m E_n(\nabla R_n)\cos(\phi_n - \phi_m)\right]$$

(The pair of indices on each summation symbol signifies a double summation over the respective indices.) This expression may be further simplified by assuming $\nabla E_l \approx \bar{0}$, i.e., the dependence of E_l on the coordinates is negligible. The phase gradient now becomes

$$\nabla\Phi_U \approx kP^{-1}\sum_{m,n} E_n E_m \cos(\phi_n - \phi_m)\hat{R}_n \tag{3}$$

If the tracking system is in the far zone of the target, then the approximation $\hat{R}_n \approx (\bar{r} - \bar{s}_n)/r$ is valid and can be used to reduce eqn. 3 to a more intuitive form.

$$\nabla\Phi_U \approx \left(\frac{k}{r}\right)\left[(x-X)\,\hat{x} + (y-Y)\,\hat{y} + (z-Z)\,\hat{z}\right] \tag{4}$$

where the coordinates of the point $Q\,(X, Y, Z)$ are given by expressions of the form

$$X = P^{-1}\sum_{m,\,n} x_n E_n E_m \cos\left(\phi_n - \phi_m\right) \tag{5}$$

The corresponding expressions for Y and Z are obtained by replacing x_n by y_n and x_n by z_n, respectively.

In the far zone, the phase gradient represents a vector normal to the surface of a sphere with center located at the point Q, see Fig. 1. The family of spheres with center at Q can be considered to be the spherical phase fronts of a field scattered by an apparent target located at Q. As a result, the point Q will define the ARC of the target and will generally not coincide with its physical centroid. Gubonin [3] and Gubonin *et al.* [4] used this far-zone expression for the phase gradient to develop a statistical model for fluctuations in the phase front of a field scattered from an extended target. However, here this expression will become an integral part of a sophisticated discrete scatterer model.

The ARC given by eqn. 5 has both range and cross-range components. The cross-range component is often associated with the familiar idea of aim-point wander while the range component is associated with the (perhaps

less familiar) phenomenon of range glint.

Finally, it is not necessary to compute the phase gradient explicitly since the ARC of the target is already given in algorithmic form by eqn. 5. To integrate this algorithm into a radar scattering code requires one to identify the, not so well defined, ensemble of scattering centers. This identification is made in the next section.

3 Scattering Center Identification

To construct a discrete scatterer model of a given target one must identify the associated ensemble of scattering centers. To facilitate this identification consider that illuminating a target with an electromagnetic field induces an electric current on the constituent components of the target and especially its surface. This induced current then becomes the source current for a secondary or scattered field. The scattered electric field can be readily expressed in terms of the source current on the target. To do so assume the target is compact and located at the origin of R^3. In that case, it is well known [11] that the electric field established by an electric current can be expressed as follows.

$$\overline{E}(\bar{r}) = i\eta k \int_{\partial V} G(\bar{r}, \bar{s}) \bullet \bar{J}(\bar{s})\, d\bar{s} \tag{6}$$

where G is the dyadic Green's function, η is the free-space wave impedance, and ∂V represents the finite support region for the induced electric current density, $\bar{J}$. The relationship between the current density and the illuminating field will be ignored for the moment. To identify the ensemble of

scattering centers for a specified target consider how that target might be represented as part of a particular simulation. In a generic sense one can imagine the constituent components of the target being tiled by a large number of small regions, denoted T_n, not necessarily identical in shape. In this manner, the support region for the electric current density can be represented as $\partial V = \bigcup_n T_n$. Using this representation, the electric field given by eqn. 6 can be rewritten as a summation over all the tiles.

$$\bar{E}(\bar{r}) = i\eta k \sum_n \left[\int_{T_n} G(\bar{r}, \bar{s}) \bullet \bar{J}(\bar{s})\, d\bar{s} \right] \tag{7}$$

To obtain an expression for the signal received by a tracking system, one must consider the polarimetric properties of the receiving antenna. In a polarization diverse tracking system the polarimetric properties of the receiving antenna are characterized in terms of a pair of polarization vectors which aid in describing the reception properties of the receiving antenna. The signal received in a particular polarization channel of the tracking system is the superposition of only those electric field components along the polarization vector and can be expressed in the following manner [12].

$$U_j(P) = (L\hat{q})_j \bullet \bar{E}(\bar{r}) \tag{8}$$

where $j = 1, 2$ distinguishes the polarization channels; each characterized by the polarization vector $(L\hat{q})_j$. The constant L_j is a normalization factor often referred to as the effective length of the receiving antenna and may be

different for each channel.

The signal received in a given polarization channel of the system is now seen to be the superposition of a finite number of elementary signals produced by the current induced on the target. This form for the received signal, given by eqn's 7 and 8, emphasizes the similarity with eqn. 1. Recall that the ensemble of scattering centers used in eqn. 1 was not well defined. Now, however, each scattering center can be associated with a well-defined region on the target surface.

$$ {}_j^e{}_n = i\eta k L_j \left[\int_{T_n} \hat{q}_j \bullet \bar{G}(\bar{r}, \bar{s}) \bullet \bar{J}(\bar{s})\, d\bar{s} \right] \tag{9} $$

The ensemble of scattering centers identified in eqn. 9 are only implicitly defined in terms of the illumination, i.e., through the action of the induced current. This expression clearly identifies the scattering centers without introducing simulation specific approximations. The implementation of eqn. 9 requires one to know the current density over the entire target, i.e., for every tile. As a result, the manner in which the current density is determined requires one to make simulation specific approximations. In the next section, several simulation specific approximations will be introduced into eqn. 9 for the purpose of demonstrating how the ARC of a target can be computed as an integral part of a radar scattering code. Several different target models will also be used to illustrate the utility of the discrete scatterer model as a tool for predicting glint induced tracking errors associated with specific radar targets.

4 Implementation and Examples

Most codes designed for predicting the scattering characteristics of radar targets fall into one of two categories: (i) those based on a method of moments procedure and (ii) those implemented using a ray casting procedure. The codes implemented using a method of moments procedure are quite accurate for computing the scattered field and hence are well suited for computing the ARC of specific radar targets. Unfortunately, tracking radar systems typically operate in the frequency range, $f > 2\text{GHz}$, for which the method of moments based codes become computationally prohibitive, especially when applied to realistic target models. As a result, the method of moments based radar scattering codes are frequently categorized as low-frequency scattering codes. Fortunately, the set of codes based on ray casting methods are well suited for efficiently computing the field scattered from electrically large complex targets, e.g., see [13]. The radar scattering codes based on ray casting techniques are often referred to as high-frequency scattering codes. Given these considerations, a high-frequency technique will be chosen for computing the ARC of a target.

4.1 Scattering Center Characterization

A high-frequency implementation of eqn. 9 is now needed for computing the target specific ensemble of scattering centers. This type of implementation can be obtained by using the following form of the far-zone approximation to the dyadic Green's function.

$$\boldsymbol{G}(\bar{r},\bar{s}) \approx g(R_n)\, e^{-i\bar{k}_n \bullet \bar{s}} (\boldsymbol{I} - \hat{R}_n \hat{R}_n) \tag{10}$$

where g is the scalar Green's function, $\bar{s}_n$ locates the centroid of T_n, I is the unit dyad, and $\bar{k}_n = k\hat{R}_n$. Using eqn. 10 in eqn. 9 gives the following simplification for e_n (the polarization index has been suppressed).

$$e_n \approx i\eta kLg(R_n)\,\hat{q} \bullet (I - \hat{R}_n\hat{R}_n) \bullet \int_{T_n} \bar{J}(\bar{s})\, e^{-i\bar{k}_n \bullet \bar{s}}\, d\bar{s} \qquad (11)$$

A relation between the induced current and the illumination is now needed. In a high-frequency code the physical optics approximation can often be used to provide that relationship, see [14, pg. 694]. In this approximation, the induced current is nonzero only on the unshaded tile, where it is defined to be $\bar{J}(\bar{s}) = 2\hat{u}(\bar{s}) \times \bar{H}(\bar{s})$ with $\hat{u}$ is the unit normal vector on the tile and $\bar{H}$ is the magnetic field illuminating the tile. When a tile is electrically small, i.e., $kT_n < 1$, the induced current is often taken to be constant over its surface. All the tile used to construct a target model will be assumed to be electrically small. Using this result in eqn. 11 gives the desired approximation that will be used to describe the ensemble of scattering centers.

$$e_n \approx \left\{ i\eta kLg(R_n) \int_{T_n} e^{-i\bar{k}_n \bullet \bar{s}}\, d\bar{s} \right\} [\hat{q} \bullet (I - \hat{R}_n\hat{R}_n) \bullet \bar{J}(\bar{s}_n)] \qquad (12)$$

Since eqn. 12 will be used as part of a simulation, it would be desirable to express eqn. 12 in closed form for computational efficiency. If the tile are flat and triangular in shape, then a closed form for eqn. 12 can be derived.

An inherent limitation in this approximation, eqn. 12, is its inability to capture the interactions that occur between the components of an extended target. This limitation is partially overcome with the use of a multibounce ray casting technique. The multibounce ray casting techniques do capture the extended interactions that result from specular scattering on an electrically large target.

4.2 Constructing the Ensemble

The scattering centers associated with a specific target are exactly those e_n that are visible to both the transmitter and receiver for a given target aspect. Constructing this ensemble amounts to determining the visibility of each tile on the target model and can be readily accomplished with a multibounce ray casting procedure. This procedure is outlined below.

The visibility of the n^{th} tile, T_n, is determined by casting a ray from the centroid of T_n toward the transmitter and similarly for the receiver. If both of these rays are unblocked by the target, then that tile becomes a scattering center in the ensemble and its scattering characteristics are determined with the use of eqn. 12. This procedure is repeated for every tile on the target and the result defines the initial ensemble of scattering centers. The initial ensemble is composed of only noninteracting scattering centers since tile-to-tile interactions are not computed.

The interacting scattering centers are created by the visible tile-to-tile interactions on an extended target. To determine these scattering centers requires a multibounce ray casting procedure. A target specific ensemble of interacting scattering centers can be constructed by using the centroid of those tile that are visible to the transmitter as ray launching points for a multibounce

ray casting procedure. At each bounce point on the target a ray is propagated into the specular direction using Snell's law, [14, pg. 187], and the visibility of the receiver is checked at every bounce point along a its path. Every bounce point visible to the receiver produces a new scattering center. The resulting ensemble can then be used to augment the initial ensemble to include specular interactions on the target.

The procedure outlined above for constructing the target specific ensemble of interacting scattering centers can be cast in the following manner.

$$U(P) = \sum_{h} \left[\sum_{n}^{N(h)} e_n^h \right] \tag{13}$$

The inner summation of eqn. 13 represents the contribution to the received signal from the scattering center ensemble defined at the h^{th} bounce of the ray casting procedure. The size of this ensemble, denoted by N, depends on the level of specular interaction being considered, i.e., h. The outer summation is over the entire ensemble that is constructed by the multibounce procedure.

4.3 Examples

To verify the simulation procedure given above, consider the one-meter diameter sphere illustrated in Fig. 2. The sphere target is ideal since the cross-range component of its associated ARC is exactly zero. The sphere model used here consists of 2,368 flat triangular tiles and for simulation purposes is only approximately spherical in shape. The tiles were assumed to represent perfect electrical conductors. Consequently, the cross-range

component of the ARC for this model will illustrate the errors associated with the entire modelling and simulation process, i.e., the errors introduced by approximating the target with a tiled model and the errors associated with the approximations used to develop eqn. 12. The cross-range component of the ARC was computed at an operating frequency of 10 GHz and in the 0^{o}-elevation plane, see Fig. 3.

The simulation and modelling error encountered when computing the ARC of this particular sphere model are quite small; being of order 10^{-5}.

An F-15 aircraft is now used to illustrate the procedure on a realistically sized model, shown in Fig. 4. The ARC of this model was computed at an operating frequency of 10 GHz. At that frequency this particular model is relatively crude, consisting of only 10,746 flat triangular tiles. These tiles were also assumed to represent perfect electrical conductors. The cross-range component of the ARC for this model was computed in an endgame scenario. In this scenario, the tracking system flies a trajectory defined along a line oriented 45^{o} counter-clockwise off of the nose of the aircraft and through a point 10 meters below the physical centroid of the target. This trajectory lies in a horizontal plane and begins 100 meters from the target. The tracking radar is modelled as monostatic with a roll-symmetric antenna pattern tilted forward 45^{o}. The ARC of the target along this trajectory is given in Fig. 5.

The glint induced tracking errors (resulting in aimpoint wander) encountered along this trajectory can be quite large and in some cases fall well outside the physical extent of the target.

5 Summary

A high-frequency multibounce radar scattering code was used as a simulation platform for demonstrating an algorithm to compute the ARC of specific radar targets. To illustrate this simulation process, several targets models were used. Simulation results for a sphere model were used to determine the errors of approximation associated with the simulation; verifying the process. The severity of glint induced tracking errors was also illustrated using a model of an F-15 aircraft. It was shown, in a deterministic manner, that the ARC of a target can fall well outside its physical extent.

Finally, the apparent radar centroid simulation based on a ray casting procedure is well suited for use on most massively parallel computing platforms and could lead to the development of a near real-time radar tracking simulation for applications such as endgame fuzing, survivability, and vulnerability analyses using specific radar targets and fuze algorithms.

6 Acknowledgment

This work was performed at Sandia National Laboratories supported by the U.S. Department of Energy under contract DE-AC04-94AL8500.

7 References

1 DELANO, R. H.: A Theory of Target Glint or Angular Scintillation in Radar Tracking', *Proc. IRE*, **41**, Dec. 1953, pp. 1778-1784.

2 SIMS, R. J. and GRAF, E. R.: 'The Reduction of Radar Glint by Diversity Techniques', *IEEE Trans.*, July 1971, **AP-19**, pp. 462-468.

3 GUBONIN, N. S.: 'Fluctuation of the Phase Front of the Wave Reflected from a Complex Target', *Radio Eng. and Electron. Phys.*, **10**, 1965, pp. 718-725.

4 GUBONIN, N. S. and CHAPURSKIY, V. V.: 'Covariance Matrix of

Coordinate Fluctuations of the Instantaneous Radar Center of a Group of Reflectors', *Radio Eng. and Electron. Phys.*, **16**, 1971, pp. 42-48.

5 BORDEN, B. H. and MUMFORD, M. L.: 'A Statistical Glint/Radar Cross Section Target Model', *IEEE Trans.*, **AES-19**, Sept. 1983, pp. 781-785.

6 SANDHU, G. S. and SAYLOR, A. V.: 'A Real-Time Statistical Radar Target Model', *IEEE Trans.*, **AES-21**, July 1985, pp. 490-507.

7 PETERS Jr., L. and WEIMER, F. C.: 'Tracking Radars for Complex Targets', *Proc. IEE*, Dec. 1963, **110**, pp. 2149-2162.

8 HOWARD, D.: 'Radar Target Angular Scintillation in Tracking and Guidance Systems Based on Echo Signal Phase Front Distortion', Proc. National Electronics Conf., Vol. 15, 1959, pp. 840-849.

9 HANSON, J. and ROBINSON, P.: 'Characterizing Angle Tracking Radars Using Complex Variables', *IEEE Trans.*, **AES-8**, Jan. 1972, pp. 35-42.

10 KING, A. S. and LEE, C. E.: 'Massively Parallel Solutions for the Modeling of Complex Electromagnetic Systems', C^3I Technology and Applications Conference, June 1992, Utica, NY.

11 CHEN, H. C.: *Theory of Electromagnetic Waves: A Coordinate-Free Approach*, (McGraw-Hill, New York, 1983), pg. 341.

12 COLLIN, R. E.: *Antennas and Radiowave Propagation*, (McGraw-Hill, New York, 1985), pg. 302.

13 VOLAKIS, J.: 'XPATCH: A High-Frequency Electromagnetic-Scattering Prediction Code and Environment for Complex Three-Dimensional Objects', IEEE Antennas and Propagation Magazine, Vol. 36, Feb. 1994, pp. 65-69.

14 BALANIS, C. A.: *Advanced Engineering Electromagnetics*, (John Wiley & Sons, New York, 1989).

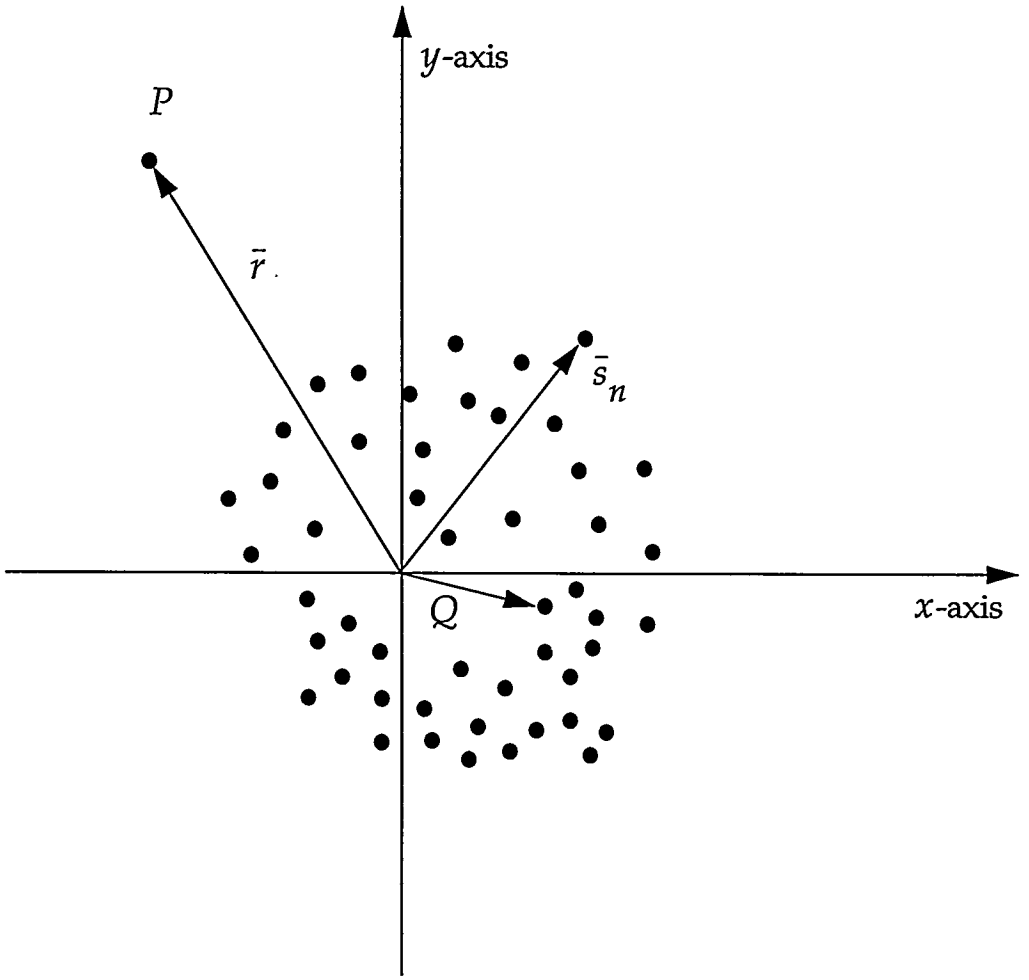

Figure 1.

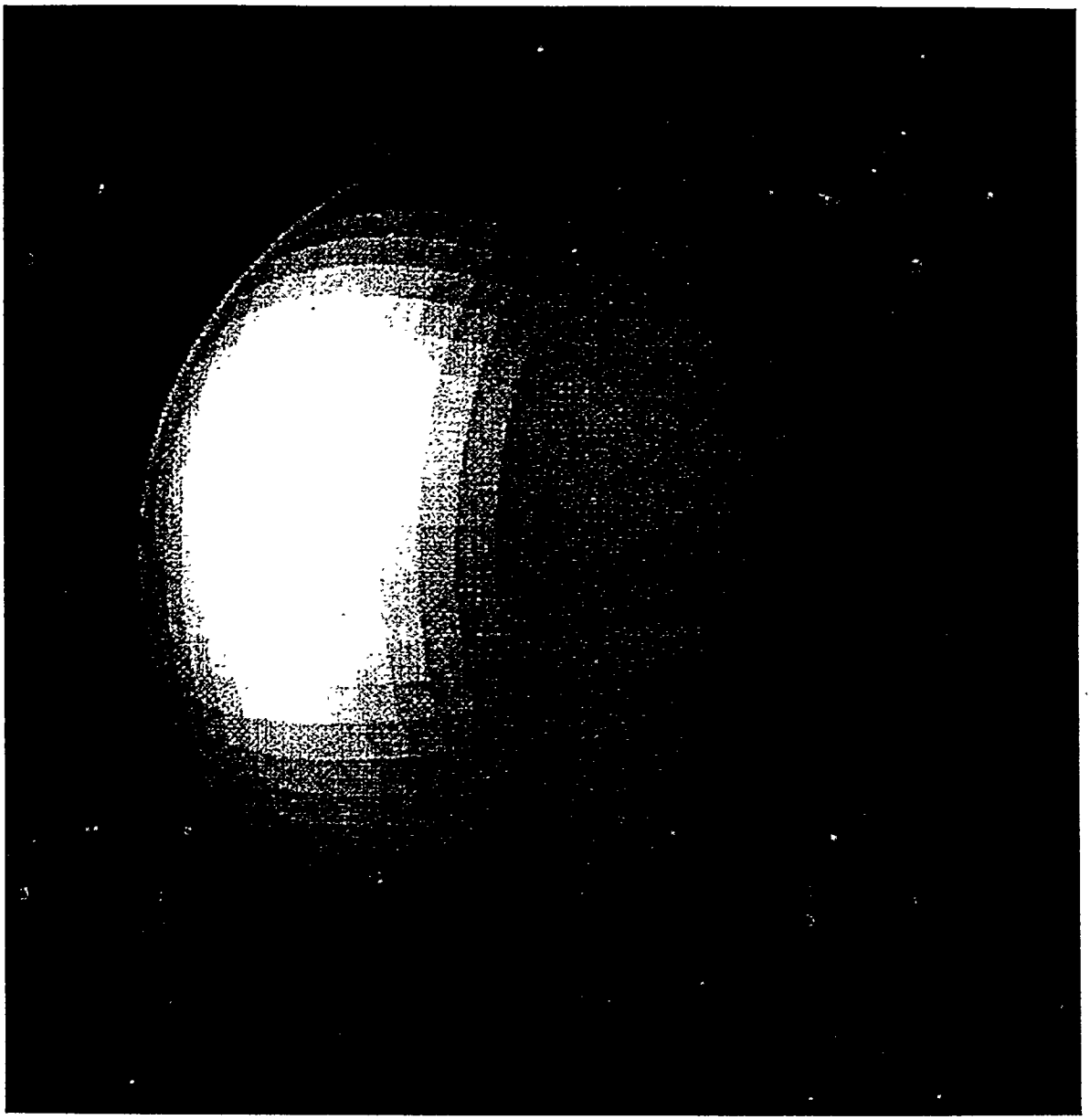

Fig. 2

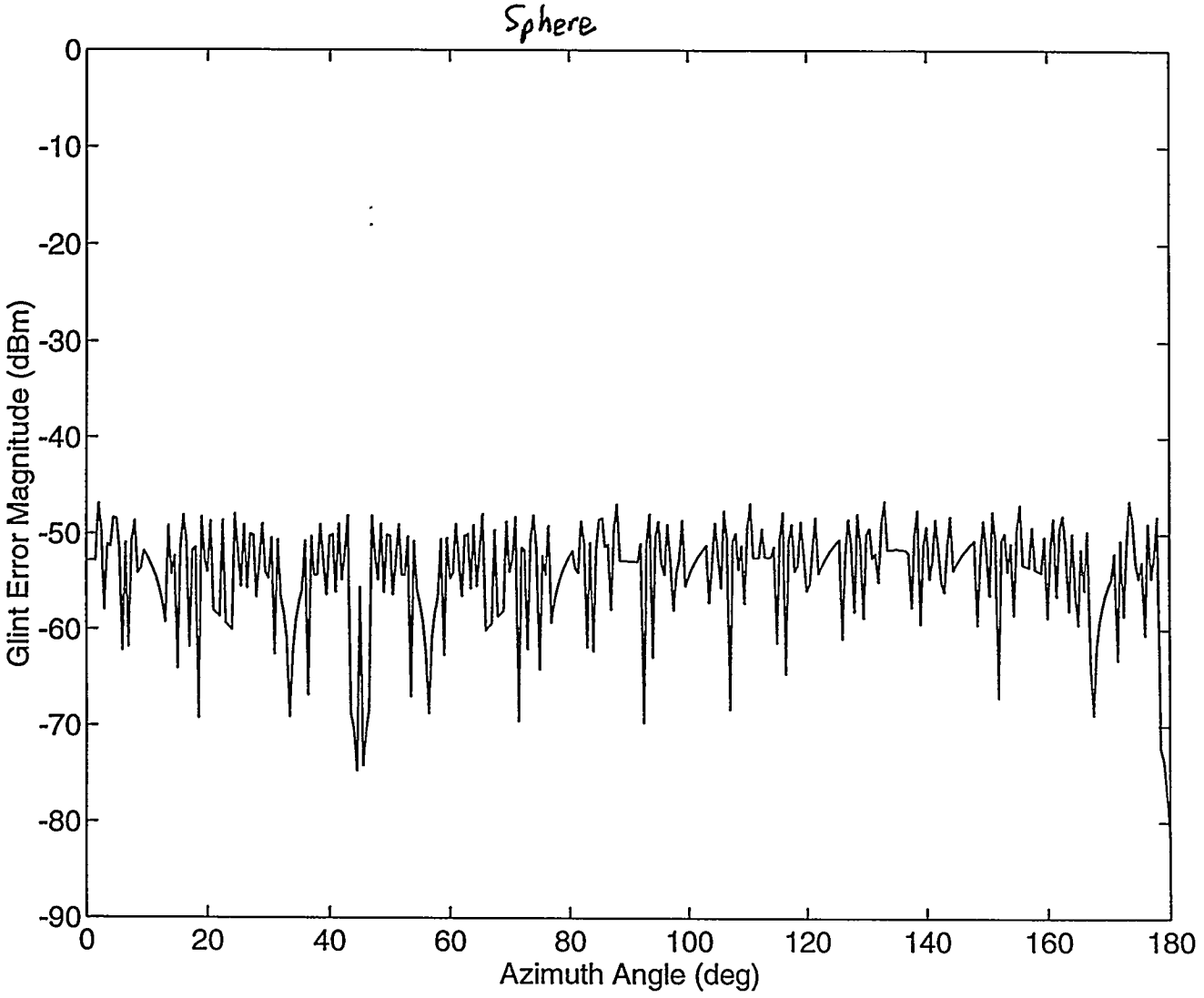
Sphere
0
-10
-20
-30
-40
-50
-60
-70
-80
-90
Glint Error Magnitude (dBm)
0
20
40
60
80
100
120
140
160
180
Azimuth Angle (deg)

Fig. 3

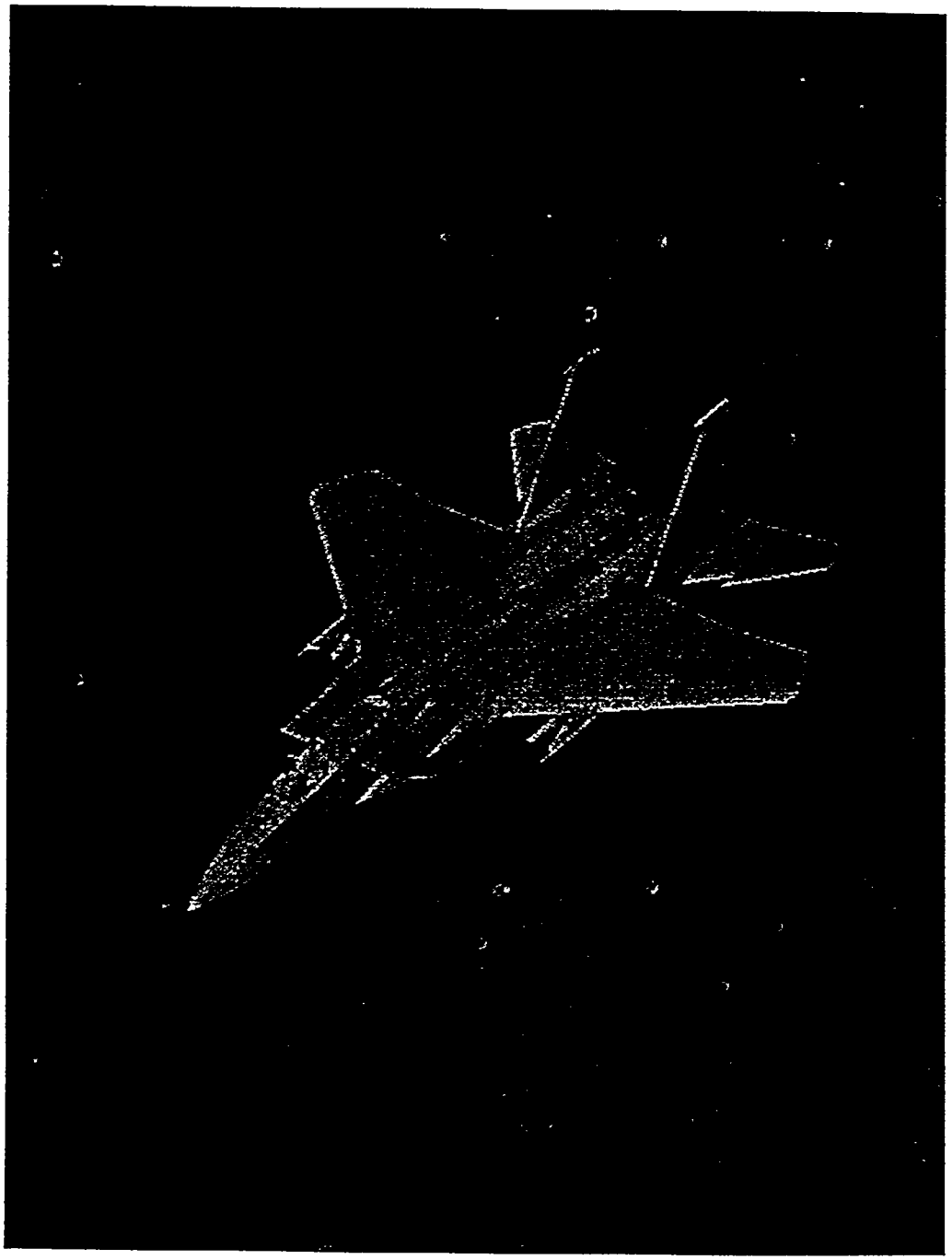

Fig. 4

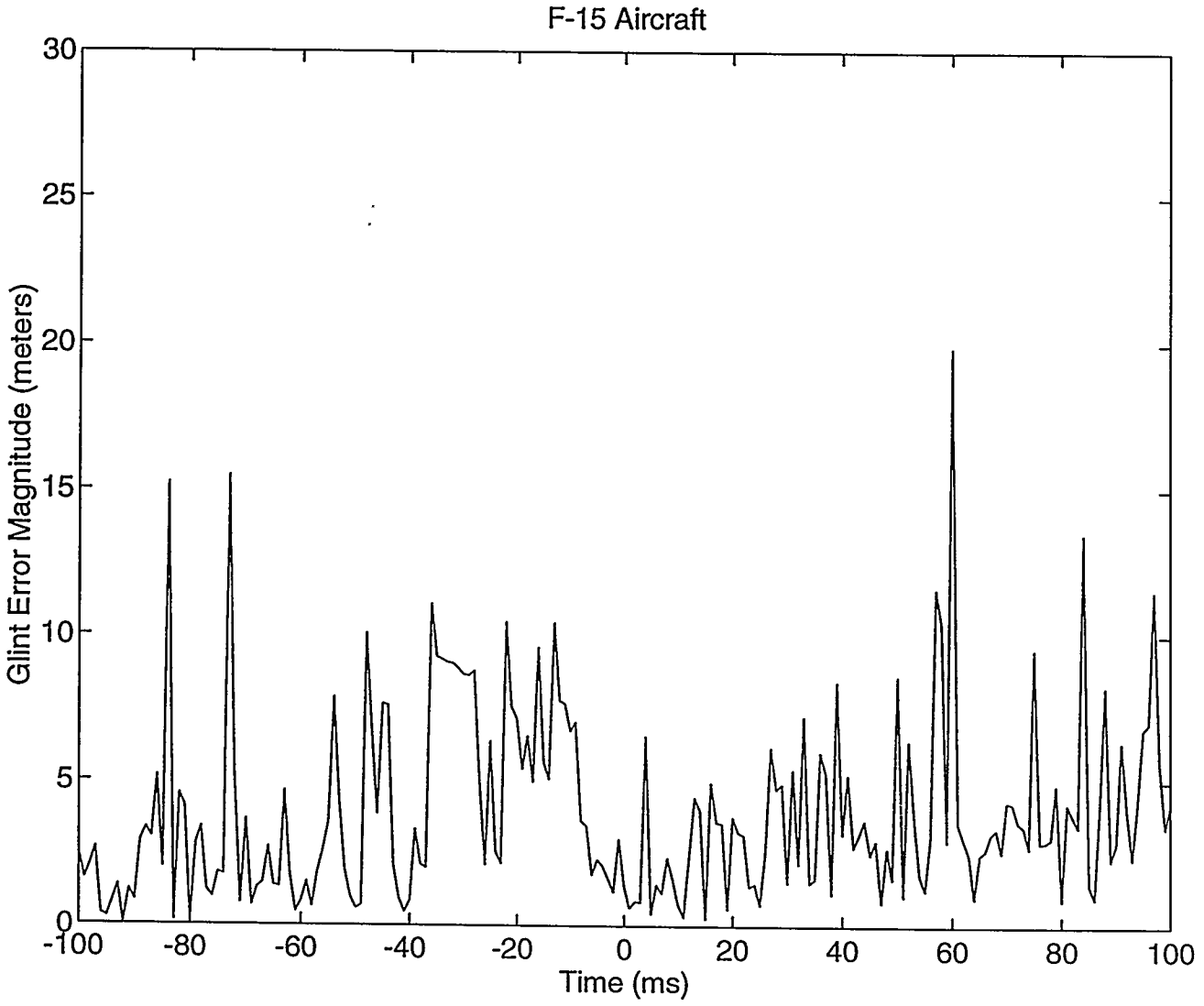

Fig. 5